STRUCTURE OF A LAYERED COMPOSITE WITH SAPPHIRE FIBERS AND MATRIX BASED ON TITANIUM AND IRON ALLOYS

Valeriy P. Korzhov, Vyacheslav M. Kiiko

Institute of Solid State Physics of the Russian Academy of Sciences, Chernogolovka city, Moscow Region, Russia

Abstract

Features of formation of multilayer structure of composite with Al_2O_3 fibres and matrix of multicomponent alloys of iron and titanium was investigated. The composite was obtained by diffusion welding under pressure of a multilayer packet composed from foils of Fe- and Ti-alloys which were alternated with fragmented Al_2O_3 fibers. It is found that during the welding process of the packet at 1200°C for 45 minutes, a titanium alloy actively interacts with the oxide fibers. The alloy is based on iron, in contrast, was completely inert with respect to sapphire. The detailed examination of the data obtained by scanning electron microscopy and X-ray analysis is presented.

Key words: *composite, metal matrix, titanium alloy, alloy of iron, diffusion welding, sapphire fiber, layered structure*

1. INTRODUCTION

Development of inhomogeneous structures for modern structural materials is predetermined by the fact that technical need to increase the operating temperature of structural elements while increasing of their specific mechanical characteristics on a traditional way of developing new alloys leads to the complete exhaustion of their resources [1]. As opposed to this situation the fibre composites with metal matrix allows to use as the metals for their advantages of crack resistance and to realize high strength, stiffness and creep resistance of some reinforcing fibers [1–3].

The single-crystal oxide fibers initially were potentially effective means for reinforcing heat-resistant metal matrix composites. Such fibers are produced from molten oxides, for example, by Stepanov's method, began to appear from the mid-1960s. However, the cost of such fibers, and fibers obtained later by other known methods such as EFG (edge-defined film-fed growth), LHFZ (laser heated floating zone directional solidification process), LHPG (laser heated pedestal growth) and μ-PD (micro pulling-down), proved to be too high to apply them in structural materials [4].

The real possibilities to use oxide fibers in composites the internal crystallization method opened [5]. A number of problems arise, the solution of which is intended to ensure receipt of the structural composite material with desired properties. The first one is to select fibers and matrix materials, providing, firstly, their interaction required during the preparation and product operation, and, secondly, the necessary properties of the composite. For example, the difference in the coefficients of thermal expansion of the matrix material and the fibers can lead to fragmentation of the fibers on lengths that do not allow them to realize the strength within the composite. The interaction between the fiber and the matrix forms the interface between them, and determines the strength of the composite and him creep resistance. Some studies of these and similar factors are given in [6–12].

For example, the "cure" of damaged oxide fibers in a matrix based on nickel and the properties of the interface fiber-matrix are discussed in [6]. It is shown that a possible decrease of the strength of fibers recovered from the matrix does not lead to a decrease in strength and creep resistance of the composite due to the effect of "healing" of surface defects of the fibers in matrix. The study of the interaction of sapphire fibers with matrices of different nickel alloys is presented in [7–8]. In particular, data on the strength of the fiber-matrix boundary in Al_2O_3/VKNA-4U composite are presented in [8]. The interface shear strength measured by «push-out» method is low, between 10-20 MPa. Such low strength of the interface does not allow enough "load" fibers of limited length and use their high strength. The creep resistance at 850–1100°C for the composite with the same fiber and matrix of

titanium aluminide obtained in liquid-phase technology is presented in [9]. The toughness, rupture strength and creep resistant of composites with matrices based on nickel aluminide and titanium aluminide, including composites with oxide fibers obtained by internal crystallization method are discussed in [10]. The interaction of sapphire fibers with a matrix based on titanium aluminide is revealed. A correlation between the results of mathematical modeling of composite structures with "insular" fiber - matrix interface and composite behavior under load with experiments on creep composites with sapphire fibers and the matrix-based on Ni–Al и Ti–Al systems is defined in [11–12].

In the proposed bibliography the present work can take an important place, as devoted to the study of the layered structure of composites of solid-phase preparation with reinforcing fragmented sapphire fibers obtained by internal crystallization method [4].

Two types of composite materials with single crystal sapphire fibers were investigated in this work. Initially composite was obtaining by diffusion welding (DW) of multilayer packet composed of foils of Fe- and Ti - alloys which alternated with fragmented sapphire fibers. But it turned out that in the process of the DW of packet titanium alloy reacted with the oxide fibers. To partially or completely reinstall the interaction of fibers with a metal matrix it was decided to build between the foils of Ti-alloy and sapphire fibers thin Al-foil and also excluding foil of Fe-alloy.

2. DESIGN AND DIFFUSION WELDING OF PACKETS

Design of 1st packet. Packet (Fe)/Al_2O_3/(Ti), consisting of foil of Fe- and Ti-alloys, contained 12 modules of three-ply sandwiches [(Fe)/(Ti)/(Fe)] and 11 (Ti)-foils (Table 1). The module is composed of the "book form" element [13], which is made of Fe-alloy foil and Ti-alloy foil embedded in the element. Before assembly, each foil of a packet of Ti-alloy was "stained" by a sticky solution of polivinilbuteral in the polyvinyl alcohol at both sides, and fragmented sapphire fibers were deposited on the surfaces of foils before solidification of solution. Here: (Fe) – 30 micron thick foil of steel grade EP678 containing 11.9 wt.%Cr, 8.9 wt.%Ni, 2.6 wt.%Ti, 1.0 wt.%Mo and the rest – Fe; (Ti) – 40 micron thick foil of Ti-alloy containing 10.0wt.%Cr, 7.4wt.%Mo, 2.7wt.%Al and the rest – Ti. The packet configuration can be written as

[(Fe)/(Ti)/(Fe)]/(Ti)/[(Fe)/(Ti)/(Fe)]/(Ti)…[(Fe)/(Ti)/(Fe)].

Thus, the total number of layers equal to 47, 24 of which were made of steel and 23 – of the titanium alloy. Between each layers (Fe) and (Ti) sapphire (Al_2O_3) fibers were placed, preferably oriented in the rolling direction of the foils. The packet dimension is 25×40 mm^2.

The design of the 2nd packet. The packet has been assembled taking into account the previous experience of making of the 1st packet design. Firstly, although the used alloys are ductility, their deformation capacity was not enough to minimize voids at the ends of the non-deformable sapphire fibers. The second, the number of sapphire layers were redundant, since at an equal thickness of fibers and foils the regularity of the composite structure distorts greatly. Conclusion is next, long fibers should be used for the formation of reinforcing oxide layers.

The second packet (Ti)/Al_2O_3/Ti) contained:

– 8 modules [(Ti)/(Al/Al_2O_3/Al)/(Ti)], which are the elements of "book form" of foil Ti-alloy, inside which there is an element of the same "book form" of Al-foil with a layer of fragmented sapphire fibers inside,

– 7 modules of the same elements of "book form" of Al-foil, and the sapphire fibers were laid between the modules.

Foils thickness of Ti-alloy and aluminium are 50 and 20 microns respectively. The orientation of fibers is close to the rolling direction of Ti-foil. The composition of the titanium alloy is the similar to Ti-alloy of the 1st packet. This packet configuration can be written as

(Ti)/(Al/Al_2O_3/Al)/(Ti)/(Al/Al_2O_3/Al)…(Ti).

Ultimately, the packet had 16 (Ti)-foils and alternating with them 15 [Al/Al_2O_3/Al] elements (see Table 1). The cross-sectional structure of the packet is represented as alternating layers of titanium and aluminum with embedded fragments of sapphire fibers in him. The package dimension is 23×35 mm^2.

Table 1. Packet structure and regimes of diffusion welding

Elements of the structure and regimes of DW	Amount of elements, *pcs*.
1. Packet (Fe)/Al_2O_3/(Ti):	
– module [(Fe)/(Ti)/(Fe)],	12
– element "book form" (Fe),	12
– segment of (Ti) -foil inside (Fe) -element,	12
– segment of (Ti)-foil between the modules.	11
Number of (Fe)-alloy layers.	12 × 2 = 24
Number of (Ti)-alloy layers.	12 + 11 = 23
Number of Al_2O_3 layers.	23 × 2 = 46
The total number of metal layers.	24 + 23 = 47
DW: 1150°C, 30 *min*, 1.5 *MPa* / 1200°C, 30 *min*, 9.8 *MPa* and 1200°, 15 *min*, 14.7 *MPa*	
2. Packet (Ti)/Al_2O_3/(Ti):	
– module [(Ti)/(Al/Al_2O_3/Al)/(Ti)],	8
– "book form" (Ti) element,	8
– "book form" (Al/Al_2O_3/Al) element of Al with Al_2O_3 layer inside module,	8
– (Al/Al_2O_3/Al) element of "book form" of Al with Al_2O_3 layer between the modules.	7
Number of (Ti)-alloy layers.	8 × 2 = 16
Number of Al-layers with sapphire fibers.	8 + 7 = 15
DW: ~600°C, 2 *h*, 12.2 *MPa* / pressure relief / 1150°C, 25 *min* without pressure and 1150°C, 5 *min*, 12.2 *MPa*	

Using of aluminium should be minimized voids at the ends of the fibers because of its good flow (1), to prevent the sapphire interaction and the metal matrix to a minimum or completely, as aluminum is a major component of sapphire and (2) to form with the alloy elements the reinforcing intermetallic layer [13–15]. Furthermore, the number of layers of Al_2O_3 in the composite was reduced by more than two times relative to the number of layers of the alloy.

Diffusion welding. 1st packet does not contain fusible components, so heating, exposure and cooling during diffusion bonding were carried out under pressure. The rate of temperature rise during heating was not limited also. DS was carried out in two stages at 1150 and 1200°C, the total time is 45 *min*, the pressure rising in steps is 1.5, 9.8 and 14.7 *MPa*.

Aluminium has a low melting temperature of 660°C. Therefore, to ensure the most complete banding aluminium in intermetallic compound $MeAl_3$ the heating of 2nd package to ~600°C was carried out in slow mode under the pressure of 12.2 MPa. It was important not to exceed the melting point of aluminium, including during subsequent 2-hour exposure of packet at this temperature. Thereafter, the pressure was released, the package is heated to 1150°C, and welding of packet was carried out without pressure at this temperature for 25 minutes. Then 5 minute exposure and cooling were under pressure 12.2 *MPa*.

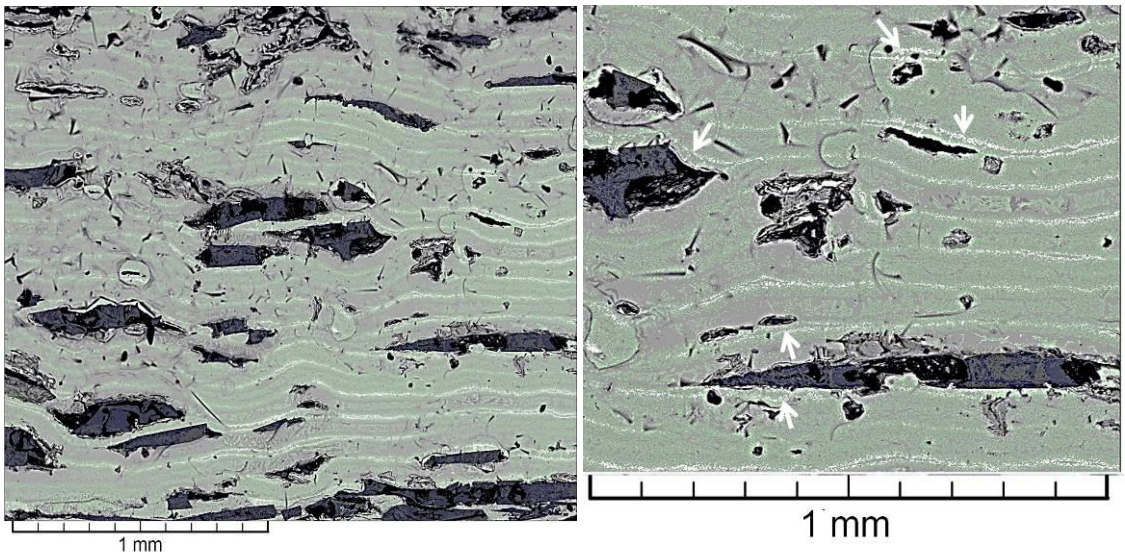
Thickness of the 1st and the 2nd packet after the DS were 2.15 and 2.00 *mm*, respectively.

3. METHODS OF STUDYING OF THE STRUCTURE

Scanning electron microscopy and X-ray spectral analysis (X-rSA) were used to study the structure of the composites. Obtaining of objects images were carried out on the digital scanning electron microscope Tescan VEGA-II and CamScan MV230 in the secondary and back-scattered electrons and by X-rSA. Both microscopes have W-cathodes and are equipped with detectors of secondary and reflected electrons and energy dispersive X-ray micro analyzer. Spectra processing of the of the characteristic X-ray was performed using the software package developed by Oxford Instruments, in which algorithm of the matrix correction PAP is included in the computational procedure [16]. Research carried out at an accelerating voltage of 20 *kV* and electron probe current of 200 *pA* on the sample of cobalt. The electron probe size is 0.16 microns.

4. (Fe)/Al_2O_3/(Ti) COMPOSITE

Microstructure. The structure of the cross section of the composite (Fig. 1) consists of a multiplicity of winding layers 65–70 microns thick with light-colored boundaries and fragmented sapphire fibres randomly embedded in them. However, it can be seen that even with relatively low magnification microscope in areas with fragments of sapphire fibers the boundaries of light tone were transformed into thin interlayers. They are shown by white arrows in Fig. 1,*b*.



a *b*

Fig. 1. The microstructure of the cross section of the composite (Fe)/Al_2O_3/(Ti) of foils of Al- and Fe-alloys with fragmented sapphire fibers after diffusion welding

At high magnification (Fig. 2) it is seen, that near the fiber the border between layers 2 are transformed into thin interlayers with a thickness of 5 to 13 microns with discrete light boundaries, indicated by white counter arrows. The interlayers are nothing else, as the remnants of Fe-alloy. The layers 2 were formed from two layers of Fe-Ti-alloys in areas of close contact between them in the diffusion bonding process and they are a combination of (Ti) + (Fe). Another picture of the interaction was observed when fiber fragment of Al_2O_3 was embedded between layers of different alloys.

It was found that in the process of DW at 1200°C sapphire actively interacts with the alloy based on titanium and one is an inert with respect to the iron-based alloy. Extensive interaction regions are formed at the point of contact of the sapphire fiber and Ti-alloy after the 45-minute exposure (Fig. 3). Similar region is presented in Fig. 2, which shows the complete absence of any interaction of the alloy based on iron which is located on the opposite side of the fiber. Moreover, this figure shows a rare case where the Ti-alloy layer is between two fragments of fibers.

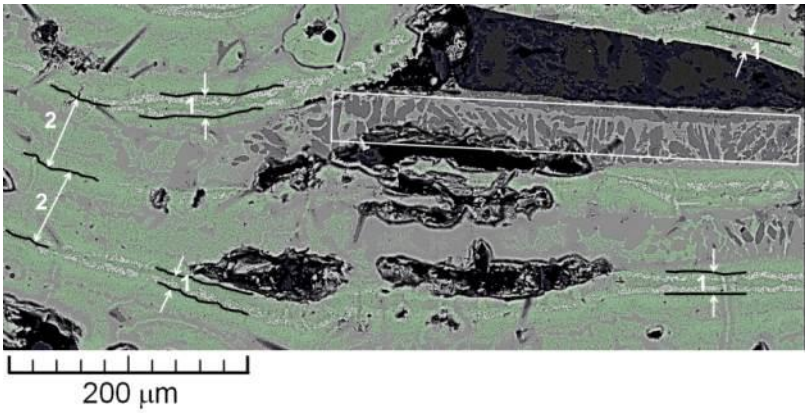


Fig. 2. The microstructure of the composite near the sapphire fragment: 1– layer between layers of (Ti) + (Fe) near the fiber; 2 – layer is formed in the process of DW of Ti- and Fe-layers; the rectangle indicates the area of interaction between the fiber and Ti-alloy

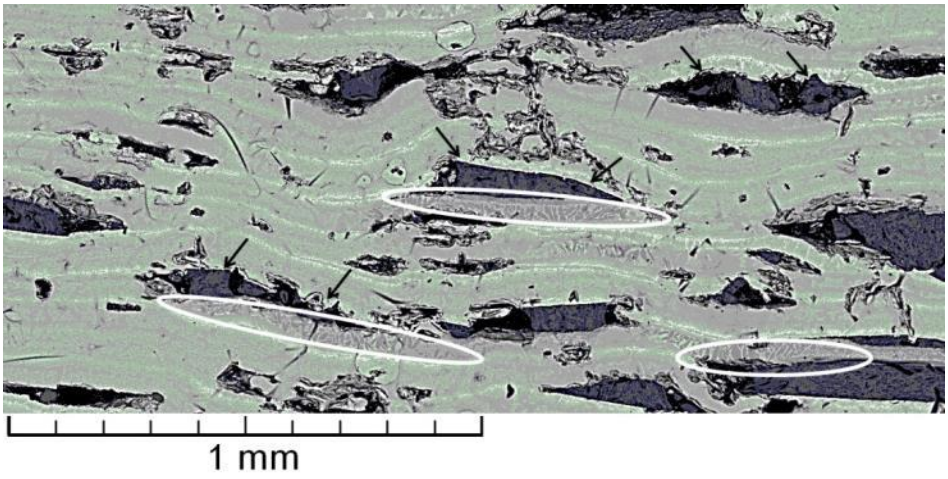


Fig. 3. Interaction zone of iron-based alloy with sapphire fibers (light contour) and the matrix areas which are inert to the fibers (black arrows)

In the diagram (Fig. 4) this place is marked by contour 1, and at a greater magnification shown in Fig. 5. Such provisions may be implemented if the two sapphire fragments at the boundaries between the

layers will appear exactly opposite each other. Then between them can become separate portion of Fe- or Ti-alloy layer.

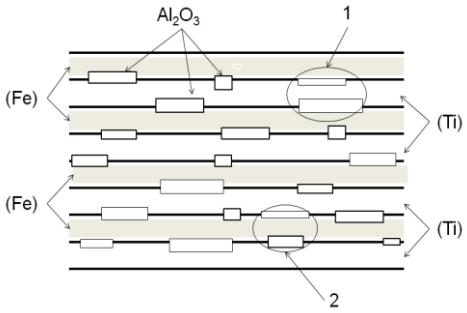


Fig. 4. Diagram is explaining how Ti- (1) or Fe-layer (2) can be between the fragments of sapphire fibers

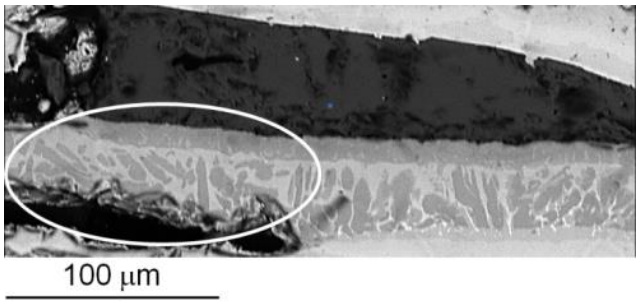


Fig. 5. The microstructure of the Ti-layer is located between the fragments of sapphire fibers (marked loop) and between the sapphire fiber and Fe-alloy layer after the DW at 1200°C for 45 minutes under a pressure of 14.7 *MPa*

Fig. 6 indicates the inertness of the alloy based on iron with respect to sapphire, it shows the unique case where over 1 mm layer of Fe-alloy does not interact with the sapphire fibers, it is located between two sapphire fibers (contour 2). Here it has a thickness of 30 *μm*. This coincides with the original foil thickness of the iron-based alloy used to make the packet assembly.

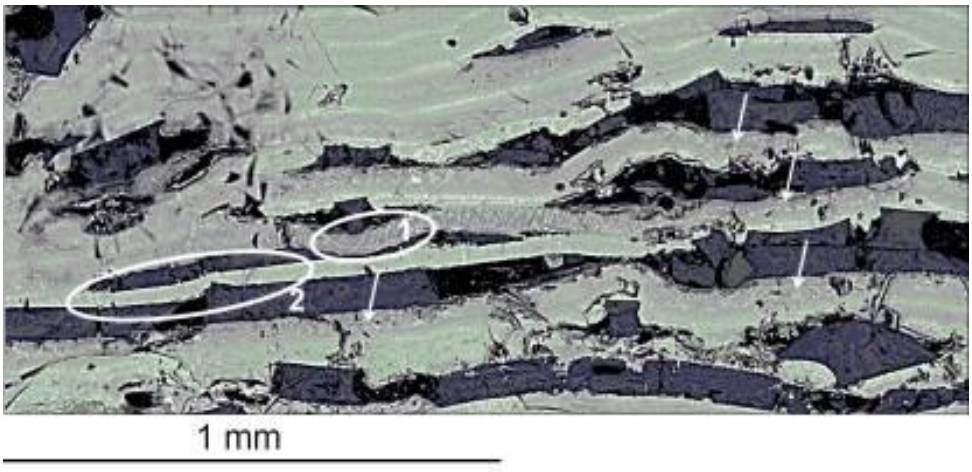


Fig. 6. The microstructure of the cross section of the packet (Fe)/Al_2O_3/(Ti) after DW: the contour 1 is a layer of an alloy based on titanium between the sapphire fibers; the contour 2 is extended area (~1 *mm*) of layer of the iron-based alloy between the sapphire fibers; arrows indicate areas of Ti alloy layer which is in contact with the fiber and Fe layer

It is seen that the layer contrast is situated between the sapphire fibers, which varies with the change of structure, but it does not change in comparison with the contrast (Fe) -layers at a distance from the fiber fragments. The situation is different with the contrast of areas of Ti-layer "sandwiched" between the fibers (contour 1) and which are in the zone of interaction with the fibers (shown by arrows). Their contrasting pattern is very different from what we see in the zones without the fibers.

X-ray analysis. Fig. 7 presents a photograph of the structure region on which X-ray analysis was carried out. Systematization of the analysis data gave the following results.

1. The spectrum 1. Sapphire fiber Al_2O_3: 40.7 at.%Al and 59.3at.%O.

2. The spectrum 2. This is the layer formed during the DW and subsequent cooling at the boundary between the sapphire fiber and layer of Ti-alloy. Its composition is 56.5 at.%Ti, 37.8 at.%Al, 4.7 at.%Cr and 1.0 at.%Mo, – from which it follows that the basic elements of formed layers are titanium and aluminium. The total content of titanium, chromium, and molybdenum is equal to 62.2 at.%. According to the constitution diagram Ti–Al it corresponds to 2-phase region of the chemical compounds Me_3Al and MeAl, where Me = Ti, Cr, and Mo, which is a solid solution of molybdenum and chromium in TiAl and Ti_3Al respectively. This two-phase layer can be considered at high magnification on Fig. 8: gray matrix of compound MeAl + needle selections in light gray contrast of Me_3Al, oriented perpendicularly to the interface between the layer Al_2O_3 and the layer Me_3Al + (Ti).

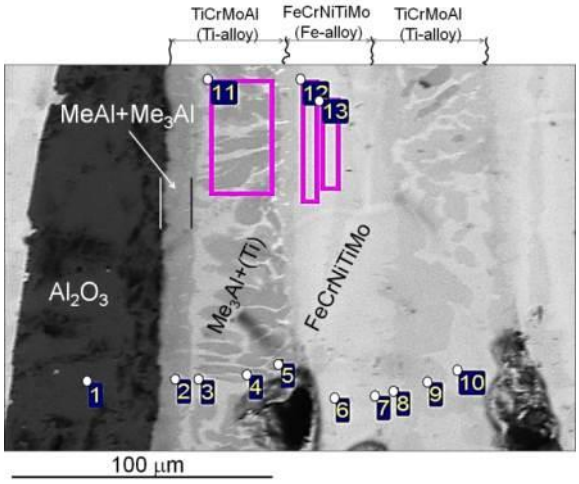


Fig. 7. The microstructure of the region where the X-ray analysis was carried out: 1–10 are spectra numbers of the local analysis; 11–13 are spectra numbers of marked regions by pink color

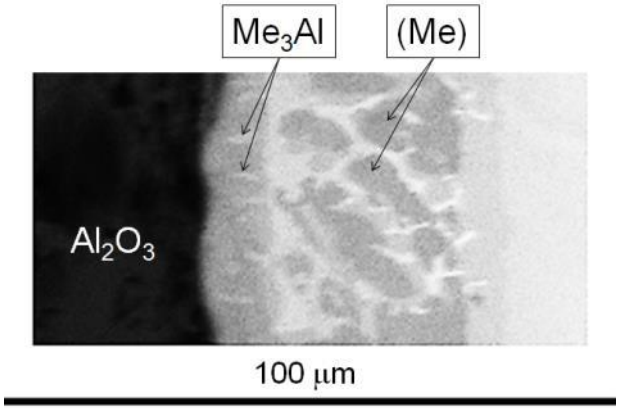


Fig. 8. The formed layers during DW and cooling at the interface of the sapphire fiber and the titanium alloy layer

3. Spectra 3, 4 and 5 represent two-phase layer of a solid solution precipitates (Ti) of gray color, these are spectra 4 and 5 in the matrix of light gray color (spectrum 3) of Me_3Al, where Me = Ti (54.9 at.%), Cr (17.8 at.%), Mo (6.7 at.%) and Fe (0.5 at.%). The total content of the Me in Me_3Al compound is 79.9 at.%, aluminium – 20.1 at.%. Content of elements in (Ti): 93.6–95.4 Ti, 3.4–4.4 Al, 0.6–1.1 Cr, 0.4–0.6 Mo and 0.1–0.2 ат.%Fe. Note that, chromium and molybdenum are present in large quantities compared with the first layer, and iron was appeared, which was not in a composition of the titanium alloy.

The kinetics of formation of the first and the second two-phase layers is represented as follows: their formation and growth occur during the DW, and the second phases are forming upon the cooling. Me_3Al is in the first layer. (Ti) is in the second one.

The spectrum 11 gives the average concentrations on area 23.5×47 μm^2 of all detected elements in the second 2-phase layer: 75.8 Ti, 12.1 Al, 8.0 Cr, 3.5 Mo, 0.4 Fe and 0.2 Ni.

Further, in order to better track the redistribution of the basic alloy (alloy forming) elements in the alloy, we present the concentration profiles of the elements depending on the range spectrum or distance, taking of zero point spectrum 1(Fig. 9).

4. Spectra 6–10 belong to the zone of solid interaction of foils of Fe-alloy EP678 grade (spectra 6–8) and Ti-alloy (spectra 10 and 9). In the zone concerning territorially to the layer of iron-based alloy iron concentration varies from 61.8 (spectrum 6) to 32.1 at.% (spectrum 8). In the zone concerning territorially to the layer of titanium-based alloy titanium concentration varies from 65.8 (spectrum 9) to 63.3 at.% (spectrum 10). Throughout the all zone of an interaction of a solid-state concentration of iron foils was decreased from 61.8 to 9.9 at.% (spectrum 10), and the concentration of titanium was increased from 12.1 (spectrum 6) to 63.3 at.%.

The boundary between the foils of various alloys after DW is not preserved of course.

5. The spectra 12 and 13 give the average concentrations on areas 5.5×46 and 6×34 μm^2 of region territorially related to the layer of iron-based alloy. As one would expect, in the greatest quantity, iron is presented here: from 52.4 to 60.6 at.%, respectively. In addition to iron, from 31.0 to 16.8 at.%Ti, 8.5 to 14.5 at.%Cr, from 4.3 to 3.7 at.%Ni, 2.4–2.6 at.% Al and 1.4–1.8 at.%Mo are presented here, respectively.

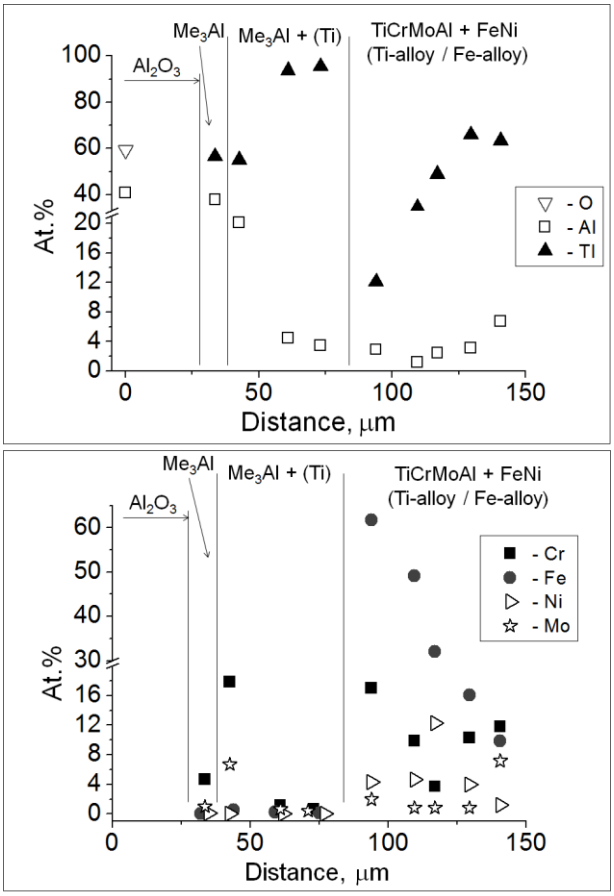


Fig. 9. The concentration profiles of the detected elements depending on the distance. For a zero point of indication accepted location of the spectrum 1

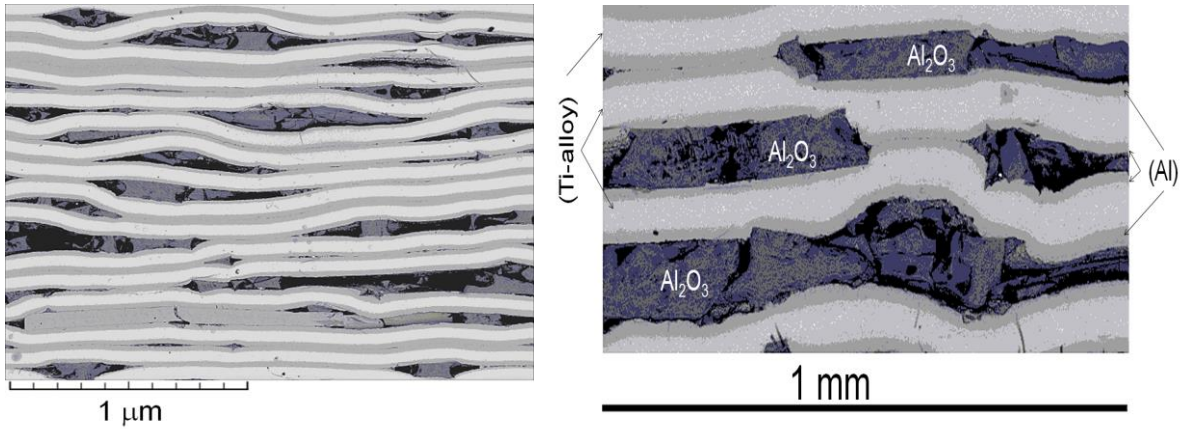
Based on these data, we can say that there are 2 independent process in the process of DW under pressure and then (within ~1 *h*) cooling at a rate of about 17 *deg./min*:

– between the foils of Ti-alloy and EP678 on the borders of Ti-alloy-EP678 their solid-phase interaction takes place with the formation of a multicomponent alloy of variable composition;

– near the sapphire fibers at the boundaries of a fiber-titanium alloy in the exposure process occurs the diffusional interaction takes place between Al_2O_3 and Ti-alloy to form a diffusion zone of layers of intermetallic compounds and MeAl and Me_3Al, which are converted into two-phase layers of MeAl + Me_3Al and Me_3Al + (Ti), respectively, in the process of cooling following the exposure.

5. (Ti)/Al_2O_3/(Ti) COMPOSITE

Macro- and microstructure. The structure of the cross section of the composite is shown in Fig. 10. It appears to be more orderly and uniform, as compared with the structure of the first composite. The alternating layers of gray and bright smoothly round the Al_2O_3 fiber embedded right in the middle layers of gray (see Fig. 10,*b*). Here the layers are designated as (Al) to mark their own the parent aluminium layers of 20 microns thick. At intervals without fibers they are merging into a single layer of double thickness of gray color. White layers are titanium alloy.



a *b*

Fig. 10. The microstructure of the cross section of the (Ti)/Al_2O_3/(Ti) composite

The composite structure is looked much more complicate at high magnification. Fig. 11 shows the microstructure of part of a typical cross-section of the composite, presenting zone without from fibers (left side of drawing) and a zone with sapphire fibers located between the (Al) layer (right side of drawing). The composite was processed by diffusion welding (see Table 1).

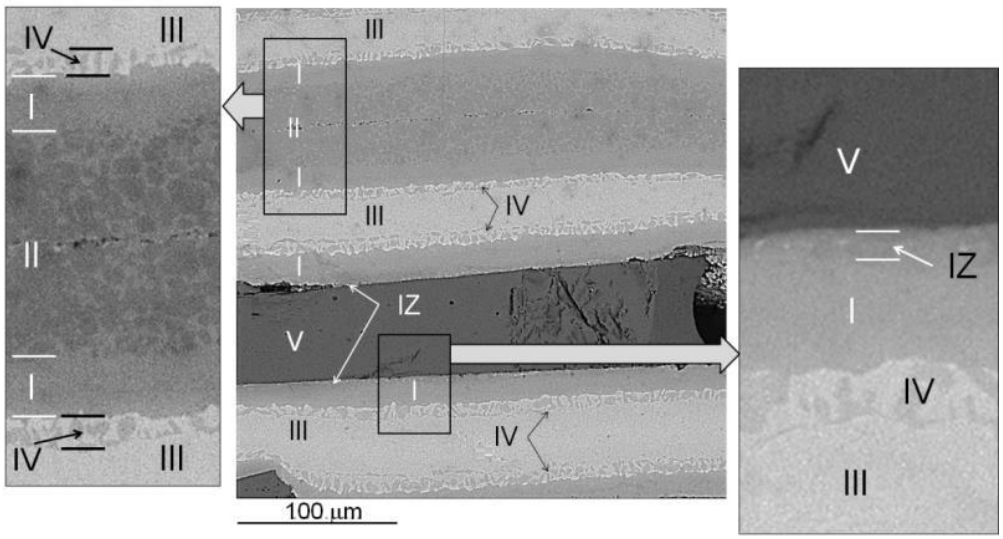


Fig. 11. The microstructure of the cross section of the (Ti)/Al_2O_3/(Ti) composite after DW

It is seen that in both zones the interaction occurred between the layers of aluminium and Ti-alloy with forming a series of diffusion layers. The aluminium layer composed of two thinner Al-layers is presented on the left fragment of cross section. After welding we can see two single-phase peripheral zones I and two-phase zone II in the middle. Changeable color contrast shows double-phase zone. The thicknesses of the peripheral layers are from 10 to 13 microns, the thickness of the middle layer is ~55 microns. Since thickness of the two Al-layers in the initial state was 40 microns, in this part of cross section the total thickness 2×I + II 2 times greater.

On the boundary of single-phase zone I with a light layer of III, which was titanium alloy before DW, it is positioned another layer of a two-phase IV thickness from 4.5 to 7.5 microns.

The same two-phase interlayer IV can be observed between light layer III and zone I, which was a single layer of aluminium before welding aluminum and which was in contact with the sapphire fiber V (see. the right side of Fig. 11). And, moreover, it should be noted that a small area of their interaction ~4.5 μm thick is at the border of Al-layer and Al_2O_3-fibre.

Identification of the layers was carried out with the help of the local X-rSA. Systematization of its data gave the following results (Fig. 12 and Tab. 2).

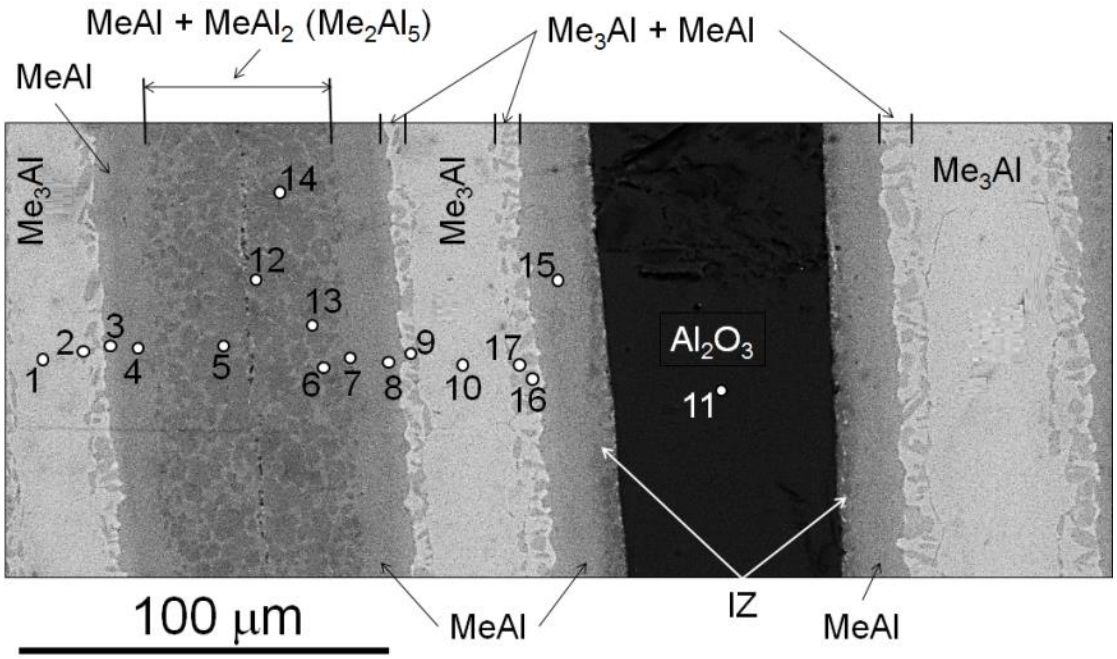


Fig. 12. The results of the local X-rS analysis: 1–17 are spectra numbers

Single-phase peripheral zones I contain 36.4 at.% aluminium, and the total concentration of all the metals (titanium, chromium, iron and molybdenum) equal to 63.7 ± 0.5 ат.%. Titanium is a fundamental element in an alloy. Therefore, as in the case of (Fe)/Al_2O_3/(Ti) composite, we followed the Ti–Al constitution diagram for layers identification. According to the diagram at 1150°C this composition lies in the region of the existence of an intermediate phase Ti_3Al, furthermore, it lies in a region with an aluminium content which exceeds him stoichiometric concentration.

Composition (36.5 at.%Me, where Me – Ti, Cr, Fe and Mo) of zone III is in a more than a similar situation where 63.5 in comparison with 50 ат.%Al.

This situation leads to the fact that compound Me_3Al decomposes partially to form a phase MeAl during cooling at the boundary of Me_3Al-MeAl and itself compound MeAl decays to form phases of $MeAl_2$ or Me_2Al_5 containing more aluminium. This explains the existence of two types of two-phase layers Me_3Al + MeAl и MeAl + $MeAl_2$ (Me_2Al_5), which have not sharp boundaries with the parent compounds Me_3Al и MeAl respectively. The two-phase layer Me_3Al + MeAl has 62.4 ± 1.5 at.%Me and 37.6 ± 0.8 at.Al, MeAl + $MeAl_2$ (Me_2Al_5) has 28.4 ± 0.5 at.%Me and 71.6 ± 1.8 at.Al.

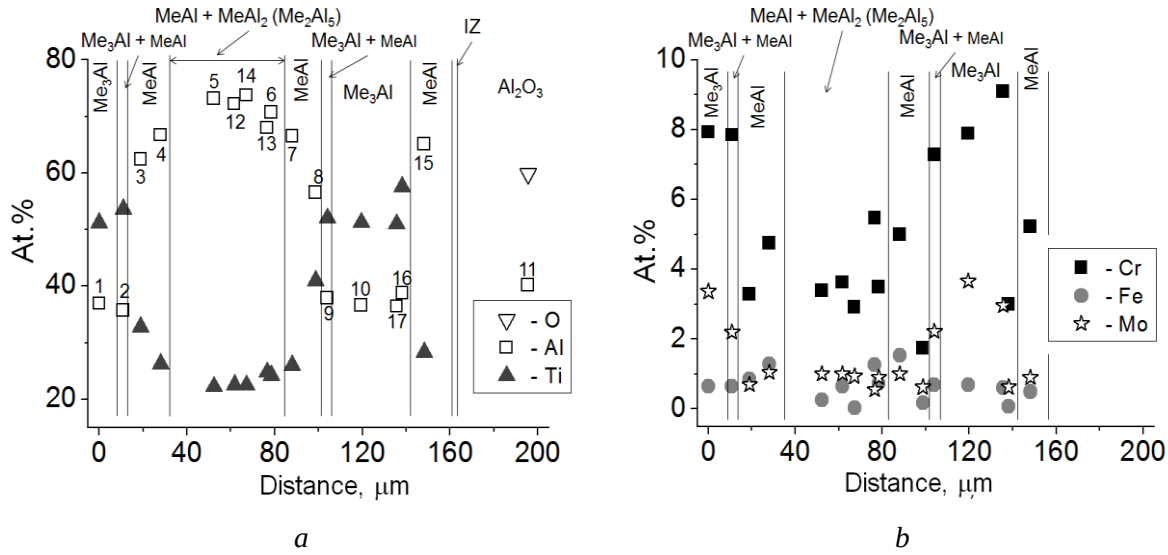
Table 2. Concentrations of elements in the layers of (Ti)/Al_2O_3/(Ti) packet formed after the DW

Spectra and layers numbers	Concentration, at.%					Identification
	Al	Ti	Cr	Fe	Mo	
I; 1, 2 and 10	36.4 ± 0.5	52.0 ± 1.1	7.9 ± 0.1	0.7 ± 0.1	3.1 ± 0.6	Me_3Al
	Me →	63.7 ± 0.5				
II; 9, 16 and 17	37.6 ± 0.8	53.5 ± 2.7	6.4 ± 2.3	0.4 ± 0.2	1.9 ± 0.9	Me_3Al + MeAl
	Me →	62.4 ± 1.5				
III; 3, 4, 7, 8 and 15	63.5 ± 3.2	30.8 ± 4.8	4.0 ± 1.2	0.9 ± 0.4	0.8 ± 0.2	MeAl
	Me →	36.5 ± 1.6				
IV; 5, 6, 12, 13 and 14	71.6 ± 1.8	23.2 ± 0.7	3.8 ± 0.7	0.6 ± 0.4	0.9 ± 0.1	MeAl + $MeAl_2$ (Me_2Al_5)
	Me →	28.4 ± 0.5				
V; 11	40.2 at.%Al and 59.8 at.%O					Al_2O_3

Note: The iron is contained as an impurity.

Aluminum content of the two-phase layers is increased, since the precipitated phase is more aluminum containing, and it should be noted that the inclusion of the second phase are located at distances comparable to the area of influence of characteristic X-ray radiation of an electron probe. Therefore, to distinguish an inclusion with greater of aluminium concentration from the primary phase matrix with lower content of aluminium is no possibility.

In addition, it may be noted that the precipitated phase contenting of lightweight aluminum more than a matrix, have a darker color in comparison with it. This is consistent with the fact that in scanning electron microscopy lightweight phase contrasts darker color if objects of two or more phases are in a structure.



a *b*

Fig. 13. Concentration dependences of aluminum, titanium and oxygen (*a*) and the chromium, molybdenum and iron (*b*): 1–17 are number of spectra. The first is number of spectrum 1

Fig. 13 shows the results of X-rSA in the form of a concentration depending on the distance. Here, the behavior of chromium, molybdenum and iron attracts attention. According to their constitution diagrams of these elements with aluminum, molybdenum and iron can form intermediate phase Me_3Al and MeAl. Chromium does not form any of them, but it does not prevent to dissolve from 7 to 9 at.% in Ti_3Al and from 3 to 5 at.% in TiAl. Molybdenum dissolves in an amount of 2–3.5 at.% in Ti_3Al and to 1 at.% in TiAl. For iron, owing to its low content, is possible only say that on the background the total content equal ~0.5 at.%, it is dissolved before 1–1.5 at.% at TiAl.

Interaction zone founded on the border of sapphire fiber intermetallic compound MeAl (see. Fig. 11 and 12), requires further experimental study. The fact that, unlike Me_3Al, MeAl compound exists at higher temperatures than 1150°C – temperature of diffusion welding of (Ti)/Al_2O_3/(Ti) packet. It is formed at ~1460°C and saved to room temperature without changing the crystalline structure.

6. CONCLUSION

1. One can no exclude that there are inert or practically inert towards the oxide fibers high temperature alloys (see, for example, the Introduction). However, the received results quite clearly show that the sapphire fibers actively interact with the used in this research titanium alloy even at temperatures of ~ 1200°C. Interaction zone spreads to the entire thickness (Ti) layer (up to 70 μm for 30 minutes of a sintering. It does not protect against this even pure aluminum layer sandwiched between the fibers and the Ti-alloy layer.

2. Also the importance of the results is as follows. Increasing of operating temperatures of alloys based on titanium inevitably leads to the use of materials based Ti–Al system containing intermetallics which have an increased strength and creep resistance. However, the presence of brittle intermetallic compounds in the structure leads to lowers the fracture toughness which is an important characteristics, considering the need of such materials also operate at low temperatures. Development of fiber composites using oxide high-strength fiber opens the possibility of solving the problem to improve balance of strength, fracture toughness and creep resistance.

3. It should also be noted that in actual conditions details of structural elements made of refractory material for a long time of operation at high temperatures condition not preclude the evolution of the structure both the matrix and interaction zone structure between the fiber and matrix in the solid phase. These results of this research contribute to the solution of this problem.

REFERENCES

1. Kelly A. Composite materials // *Nauka – proizvodstvu*, 2007, №2(95), pp. 1–9 (in Russian).
2. Svetlov I.L. High-temperature Nb–Si composites // *Materialovedenie*, 2010, №9, pp. 29–38 and №10, pp. 18–27 (in Russian).
3. Mileiko S.T. The future of composites and composite science // *Nauka – proizvodstvu*, 2007, №2(95), pp. 10–24 (in Russian).
4. Kurlov V.N., Kiiko V.M., Kolchin A.A., Mileiko S.T. Sapphire fibres grown by a modified internal crystallization method // *J. Crystal Growth*, 1999, vol. 204, pp. 499–504.
5. Mileiko S.T and Kazmin V.I. Crystallization of fibres inside a matrix: a new way of fabrication of composites // *J. Mater, Sci.*, 1992, vol. 27, pp. 2165–2172.
6. Mileiko S.T., Sarkissyan N.S., Kolchin A.A., Kiiko V.M. Oxide fibres in a nikel-base matrix – do they degrade or become stroner? // *J. Materials: Design and Application*, 2004, vol. 218, pp. 193–200.

7. Mileiko S.T., Kiiko V.M., Kolchin A.A., Serebryakov A.V., Korzhov V.P., Starostin M.Yu., Sarkissyan N.S. Oxide-fibre/Ni-based matrix composites – part I: fabrication and microstructure // *Composites Science and Technology*, 2002, vol. 62, no. 2, pp. 167–179.
8. Mileiko S.T., Kiiko V.M., Kolchin A.A., Korzhov V.P., Prokopenko V.M. Oxide-fibre/Ni-based matrix composites – part II: mechanical behavior // *Composites Science and Technology*, 2002, vol. 62, no. 2, pp. 181–193.
9. Mileiko S.T., Povarova K.B., Korzhov V.P., Serebryakov A.V., Kolchin A.A., Kiiko V.M., Starostin M.Yu., Sarkissyan N.S., Antonova A.V. High-temperature creep of sapphire-fibres/titanium-aluminide-matrix composites // *Scripta Materialia*, 2001, vol. 44, no. 10, pp. 2463–2469.
10. Povarova K.B., Kazanskaya N.K., Drozdov A.A., Antonova A.V. Heat-resistant composites with intermetallic matrix // *Nauka – proizvodstvu*, 2007, №2(95), pp. 36–52 (in Russian).
11. Mileiko S.T., Kiiko V.M. High temperature creep of metal matrix composites under variable loadings // *Mechanics of Composites Materials*, 2004, vol. 40, no. 4, pp. 523–534 (in Russian).
12. Mileiko S.T., Kiiko V.M., Khvostunkov K.A. Creep of composites with a porous/matrix interface under variable loading // *Theoretical and Applied Mechanics*, 2006, vol. 45, pp. 41–45.
13. Korzhov V.P., Karpov M.I., Zheltyakova I.S. Changes in the structure and heat resistance of multilayer titanium-aluminum composite obtained by diffusion in solid phase // *Scientific Proceedings of the Scientific-Technical Union of Mechanical Engineering*, XXIII, vol. 22/185, September 2015, pp. 104–108.
14. Korzhov V.P., Karpov M.I., Prokhorov D.V. Multilayer heat-resistant materials based on intermetallic compounds of niobium and titanium: preparation, structure and mechanical properties // *Scientific Proceedings of the Scientific-Technical Union of Mechanical Engineering*, XXI, vol. 10/147, September 2013, pp. 120–123.
15. Karpov Mikhail I., Korzhov Valery P., Prokhorov Dmitry V., Zheltyakova Irina S., Stroganov Tatiana S., Vnukov Victor I. Preparation, structure and high temperature properties of layered Nb/Al- and Ti/Al-composites // *J. Intern. Scient. Public.: Materials, Methods and Technologies*, vol. 8, 2014, pp. 177–185.
16. Pouchou J.L., Pichoir F. A new model for quantitative X-ray microanalysis. I. Application to the analysis of homogeneous samples // *Recherche Aerospatiale*, 1984, vol. 3, pp. 13–38.